Effects of amotosalen treatment on human platelet lysate bioactivity

Christian Christensen[1,2,3], Sandra Mjoll Jonsdottir-Buch[1,2,3], Olafur Eysteinn Sigurjonsson[1,2,3,4*]

[1] The Blood Bank, The National University Hospital of Iceland, Reykjavik, Iceland

[2] Faculty of Medicine, Biomedical Center, University of Iceland, Reykjavik, Iceland

[3] Platome Biotechnology, Hafnarfjörður, Iceland

[4] School of Science and Engineering, University of Reykjavik, Reykjavik, Iceland

* Corresponding author

E-mail: oes@landspitali.is (OES)

Abstract

Background: Clinical application of mesenchymal stromal cells (MSCs) usually requires an *in vitro* expansion step to reach clinically relevant numbers. *In vitro* cell expansion necessitates supplementation of basal mammalian cell culture medium with growth factors. To avoid using supplements containing animal substances, human platelet lysates (hPL) produced from expired and pathogen inactivated platelet concentrates can be used in place of fetal bovine serum. Due to lack of experience and global diversity in bacterial detection strategies, most transfusion units are currently not pathogen inactivated. As blood banks are the sole source of platelet concentrates for hPL production, it is important to ensure product safety and standardized production methods. To achieve these aims, we assessed the quality of hPL produced from expired platelet concentrates with pathogen inactivation applied after platelet lysis, as well as its ability to support MSC proliferation and tri-lineage differentiation.

Methodology/principal findings: Bone marrow-derived MSCs (BM-MSCs) were expanded and differentiated using hPL derived from pathogen inactivated platelet lysates (hPL-PIPL), with pathogen inactivation applied after lysis of expired platelets. Results were compared to those using hPL produced from conventional expired pathogen inactivated human platelet concentrates (hPL-PIPC), with pathogen inactivation applied after soon after blood donation. hPL-PIPL treatment had lower concentrations of soluble growth factors and cytokines than hPL-PIPC treatment. When used as supplementation in cell culture, BM-MSCs proliferated at a reduced rate, but more consistently, in hPL-PIPL than in hPL-PIPC. The ability to support tri-lineage differentiation was comparable between lysates.

Conclusion/significance: These results suggest that functional hPL can be produced from expired and untreated platelet lysates by applying pathogen inactivation after platelet lysis. When carried out post-expiration, pathogen inactivation can provide a valuable tool to further standardize global hPL

41 production methods, increase the pool of starting material, and meet the future demand for animal-free
42 supplements in human cell culturing.

43

Introduction

Pathogen inactivation systems are proactive alternatives to conventional bacterial screening and prevention methods for blood transfusion products [1]. Several systems are currently available on the market such as the INTERCEPT™ Blood System, Mirasol™ and THERAFLEX™ [2]. The INTERCEPT™ Blood System for pathogen inactivation of platelets gained the CE mark in 2002 [3] and is routinely used in several European countries [4]. The system effectively reduces the accumulation of pathogens by blocking their ability to replicate [3]. The active compound used in the INTERCEPT System, amotosalen S-59, passes through cell membranes, bacterial walls, and viral envelopes and intercalates between helical regions of DNA and RNA [5]. Covalent crosslinks are formed between amotosalen S-59 and pyrimidine bases upon exposure to UV-A illumination, leaving pathogenic organisms unable to replicate [3].

Implementing a pathogen inactivation system improves the safety of transfusion units and allows platelets to be stored for an extended period of up to seven days [3]. Blood banks must stock surplus transfusion units; with approximately 2 million reported annual platelet transfusions in the United States alone [6], this inevitably results in large quantities of expired platelets [7]. Although expired platelet concentrates are unfit for transfusion medicine due to safety concerns, their abundance of growth factors makes them suitable for use in cell cultures [8].

Human mesenchymal stromal cells (MSCs) are multipotent cells capable of undergoing *in vivo* differentiation into end-stage cell types of connective tissues [9]. They were initially described, in the 1960s, as plastic-adherent and fibroblast-like cells with clonogenic potential *in vitro* [10]. Today, they are recognized as a part of stem cell niches in the bone marrow [11] and are known to play a role in immunomodulation [12], as demonstrated by the prominent contribution of the cells in reversing graft-versus-host-disease [13]. Scientific interest in MSCs has developed in recent years, making them one of the most-studied human cell types related to cell-based therapy [14].

An *in vitro* expansion step is usually necessary to attain clinically relevant numbers of MSCs [15]. Successful expansion of MSCs requires that basal cell culture medium be supplemented with a source of mitogens, such as growth factors. To date, this has mostly been performed using fetal bovine

serum (FBS), which contains low amounts of immunoglobins and complement factors [16]. However, concerns regarding the content of animal components and large lot-to-lot variability has initiated a quest for replacements [16–18]. Platelet derivatives such as human platelet lysates (hPL) are currently considered promising replacements for FBS [8,19–22] due to their non-xenogeneic nature and abundance of growth factors [23]. hPL has successfully been produced from fresh platelets [24], expired platelets [8], and, most recently, from expired and pathogen inactivated platelets [22]; all have been found to either be comparable to or to outperform FBS.

hPL is commonly manufactured by exposing platelet concentrates to repetitive cycles of freezing and thawing, resulting in degranulation [21], but it can also be produced by $CaCl_2$ activation [25], sonication [26], or by using a solvent/detergent strategy [27]. Degranulation causes the α-granules to release growth factors and cytokines into solution [28]. To obtain a sufficient volume of hPL, allogeneic hPL are typically pooled using up to 120 donors [29]; however, recent research has demonstrated that pooling can be done effectively using up to 250 donors [30]. The end product is refined by centrifugation and sterile filtration to remove platelet fragments [29].

Recently, emphasis has been placed on improving standardization in global good manufacturing practice (GMP)-grade hPL production, as current production methods vary between manufacturers [31]. Although pathogen inactivation techniques have recently been introduced into the preparation of transfusion products, they are predominantly applied in Europe, while blood banks in the United States and Asia primarily rely on bacterial screening systems such as BacT/ALERT to ensure product safety [32]. As a result, most platelets used for hPL production are currently not pathogen inactivated.

In this study, hPL from pathogen inactivated platelet lysates (hPL-PIPL) was compared to hPL produced from conventional pathogen inactivated platelet concentrates (hPL-PIPC). We evaluated and compared the total protein content and concentrations of selected soluble growth factors and cytokines between hPL-PIPL and hPL-PIPC. Furthermore, we compared long-term proliferation and tri-lineage differentiation of bone marrow-derived MSCs using hPL-PIPL and hPL-PIPC as cell culture media supplements.

Results

Growth factor and cytokine concentrations are lower in hPL-PIPL than in hPL-PIPC

Quantification of 37 soluble growth factors and cytokines was performed using Luminex xMAP technology following platelet lysate production. Each of the measured growth factors and cytokines was present at lower concentrations in hPL-PIPL than in hPL-PIPC (Table 1). The mean decreases for all evaluated growth factors and cytokines in hPL-PIPL (as compared to hPL-PIPC) for two produced batches were 29 ± 15% ($p < 0.001$) and 36 ± 19% ($p < 0.001$). The mean differences between hPL-PIPL and hPL-PIPC in key growth factors for the two batches ranged from 4.2 to 36%: PDGF-AB/BB (4.2 ± 1.8%); PDGF-AA (12 ± 17%), EGF (23.9 ± 7.8%); VEGF (26.6 ± 0.62%); and FGF-2 (36.3 ± 1.8%).

110 **Table 1. Growth factor and cytokine concentrations in two batches of undiluted hPL.**

	Batch 23			Batch 24			Batch 23 vs. Batch 24
Growth Factor / Cytokine	hPL-PIPC pg/mL	hPL-PIPL pg/mL	Difference[a] %	hPL-PIPC pg/mL	hPL-PIPL pg/mL	Difference %	Mean ± SD[b] %
EGF	1992	1361	32	346	291	16	22.9 ± 7.8
Eotaxin	96	53	45	129	88	32	38.2 ± 6.7
FGF-2	517	320	38	478	313	34	36.3 ± 1.8
Fractalkine	234	196	16	164	105	36	26 ± 10
G-CSF	49	27	44	57	27	53	48.5 ± 4.1
GM-CSF	27	20	26	27	14	48	37 ± 11
IFNα2	76	49	35	84	44	47	41.2 ± 6.2
IFNγ	14	12	19	14	8.5	40	29 ± 11
IL-1α	59	50	16	29	19	35	25.4 ± 9.6
IL-1β	5.5	3.4	38	6.4	2.6	59	48 ± 11
IL-1RA	503	452	10	1030	884	14	12.2 ± 2.0
IL-2	7.8	6.1	23	4.0	1.8	55	39 ± 16
IL-3	6.3	4.3	32	6.2	3.1	49	40.6 ± 8.4
IL-4	31	17	47	48	27	44	45.5 ± 1.1
IL-5	34	28	16	82	69	16	15.7 ± 0.0
IL-6	13	7.9	40	12	3.3	72	56 ± 16
IL-7	30	20	32	36	22	40	36.4 ± 3.9
IL-8	50	38	24	76	64	16	19.9 ± 3.8
IL-9	10	7.2	29	6.5	3.9	39	34.3 ± 5.0
IL-10	20	14	30	7	2.4	65	48 ± 18
IL-12p40	61	51	16	62	32	49	33 ± 16
IL-12p70	11	6.2	44	12	6.2	47	45.5 ± 1.5
IL-13	183	176	3.7	433	372	14	8.8 ± 5.2
IL-15	12	6.6	45	8.6	3.6	59	51.6 ± 7.1

IL-17A	14	14	4.1	10	5.5	43	23 ± 19
IP-10	120	58	52	101	51	49	50.7 ± 1.4
MCP-1	157	111	30	185	157	15	22.4 ± 7.4
MCP-3	301	276	8.3	520	491	5.7	7.0 ± 1.3
MDC	705	192	73	754	230	69	71.1 ± 1.7
MIP-1α	24	22	11	33	30	8.8	9.8 ± 1.0
MIP-1β	123	82	34	165	127	23	28.4 ± 5.4
PDGF-AA	15850	11232	29	9105	9548	-4.9	12 ± 17
PDGF-AB/BB	27802	27146	2.4	25157	23661	5.9	4.2 ± 1.8
TGF-α	3.0	1.8	40	4.1	1.9	53	46.5 ± 6.5
TNFα	24	16	35	26	15	42	38.5 ± 3.5
TNFβ	266	236	11	570	490	14	12.7 ± 1.4
VEGF	538	392	27	441	327	26	26.6 ± 0.6
Mean ± SD (%)			29 ± 15			36 ± 19	32 ± 16
p-value[c]			< 0.001			< 0.001	< 0.001

[a] Difference (%) between hPL-PIPC and hPL-PIPL within individual batches (Batch 23 and Batch 24). Note that the concentrations for all growth factors and cytokines were lower in hPL-PIPL.

[b] Mean ± SD (%) represents the mean difference between hPL-PIPC and hPL-PIPL for both batches (n = 4).

[c] p-values are reported on the overall differences between treatments (hPL-PIPC and hPL-PIPL) in individual batches (23 and 24) and for both batches combined. p-values were determined using a paired ratio t-test.

Proliferation of MSCs in hPL-PIPL is comparable to, but slower than, that in hPL-PIPC

Proliferation of MSCs originating from the bone marrow of two individual donors were assessed during nine cell passages (Fig 1). Cumulative population doublings (CPDs) were assessed from passage 4 through passage 9. MSCs grown in cell culture media supplemented with hPL-PIPL (hPL-PIPL-MSCs) proliferated significantly slower than hPL-PIPC-MSCs ($p < 0.001$) from passage 5 through passage 9. At the end of passage 9, MSCs from Donor 6 had reached 19.42 ± 0.10 CPDs and 21.25 ± 0.03 CPDs with hPL-PIPL and hPL-PIPC supplementation, respectively, and MSCs from Donor 13 had reached 10.50 ± 0.40 CPDs and 12.80 ± 0.20 CPDs.

Fig 1. Long-term proliferation of MSCs, expressed as cumulative population doublings. Proliferation of MSCs from two donors (D6 and D13) was evaluated in cell culture media supplemented with hPL-PIPC or hPL-PIPL after passage 3 (indicated by the vertical dotted line). Points represent mean ± SEM at the end of each passage (n = 6 cell cultures per passage, assessed in two independent experiments). Asterisks (* $p < 0.05$) indicate statistical significance between hPL-PIPC and hPL-PIPL for an individual donor, evaluated via a two-way ANOVA with Tukey's post hoc test.

Tri-lineage differentiation is not affected by the timing of pathogen inactivation

hPL-PIPL-MSCs were successfully differentiated into osteogenic, adipogenic and chondrogenic lineages. Osteogenic differentiation was evaluated during 28 days of stimulation in osteogenic media. Alkaline phosphatase (ALP) activities in both hPL-PIPL-MSCs and hPL-PIPC-MSCs were significantly elevated after seven days as compared to unstimulated control cultures ($p < 0.05$) (Fig 2). A peak in ALP activity was observed at day 14 for both hPL-PIPL-MSCs (3.6 ± 0.1 nmol (p-nitrophenol)/min)

and hPL-PIPC-MSCs (3.8 ± 0.1 nmol (p-nitrophenol)/min), followed by fairly consistent ALP activity between days 14 and 28. Comparable mineralization between hPL-PIPC and hPL-PIPL MSCs was demonstrated by Alizarin Red S staining after 28 days of differentiation (Figs 3A and B).

Fig 2. Alkaline phosphatase activity during osteogenic differentiation. MSCs were differentiated in osteogenic media supplemented with hPL-PIPL or hPL-PIPC, with MSCs grown in expansion media included as a control. Points represent means ± SEM (n = 6 cell cultures per timepoint, assessed in two independent experiments). Asterisks (* $p < 0.05$) indicate statistical significance versus the control, evaluated via a two-way ANOVA with Tukey's post hoc test.

Fig 3. Tri-lineage differentiation of MSCs. MSCs differentiated using hPL-PIPC are shown in A, C, and E, while MSCs differentiated using hPL-PIPL are shown in B, D, and F. A and B show Alizarin Red S staining, used to demonstrate mineralization (black arrows) after 28 days of stimulation in osteogenic medium. C and D show Oil Red O staining, used to demonstrate accumulation of lipid droplets (black arrows) after 14 days of stimulation in adipogenic medium. E and F show Masson's trichrome staining, used to demonstrate collagen fibers (black arrows) and lacunae formation (yellow arrows) after 35 days of chondrogenic stimulation.

Adipogenic differentiation was evaluated during 14 days of stimulation in adipogenic media. Accumulation of lipid droplets in the cell periphery was confirmed by positive Oil Red O staining after 7 days. After 14 days of differentiation, lipid droplets were distributed throughout the cells (Figs 3C and D).

Chondrogenic differentiation was evaluated during 35 days of stimulation in chondrogenic media. After 28 days of differentiation, the concentration of glycosaminoglycans (GAGs) was significantly higher ($p < 0.05$) in cell pellets supplemented with both hPL-PIPC and hPL-PIPL than in unstimulated control cell pellets (Fig 4). GAG concentration remained significantly higher than the control during differentiation of hPL-PIPC-MSCs at day 35 ($p < 0.05$), while GAG concentration decreased again in hPL-PIPL-MSCs by day 35 such that there was no longer a significant difference from the control. No statistically significant differences were observed between hPL-PIPC-MSCs and hPL-PIPL-MSCs. Lacunae formation and accumulation of collagen fibers were demonstrated after 35 days of differentiation using Masson's trichrome staining (Figs 3E and F).

Fig 4. Concentration of glycosaminoglycans. GAG concentration was measured in MSC pellets stimulated with chondrogenic media supplemented with either hPL-PIPC or hPL-PIPL. Pellets grown in expansion media were included as a control. Points represent mean ± SEM ($n = 2$ pellets per timepoint, assessed in two individual experiments). Asterisks (* $p < 0.05$) indicate statistical significance versus the control, evaluated via a two-way ANOVA with Tukey's post hoc test.

Discussion

In this study, hPL derived from pathogen inactivated platelet lysates (hPL-PIPL) was compared to conventional hPL derived from pathogen inactivated platelet concentrates (hPL-PIPC). We evaluated the composition of the lysates as well as their applicability for use as supplements to support BM-MSC proliferation and tri-lineage differentiation.

Concentrations of all 37 selected soluble growth factors and cytokines were significantly reduced in hPL-PIPL compared to hPL-PIPC, with an average difference of 32 ± 16% ($p < 0.001$). Of the key growth factors, we found that the differences between hPL-PIPC and hPL-PIPL in PDGF-AB/BB and PDGF-AA were relatively small, at 4.2 ± 1.8% and 12 ± 17%, respectively. The effects on EGF, VEGF, and FGF-2 were slightly higher, with observed reductions in hPL-PIPL of 23.9 ± 7.8%, 26.57 ± 0.62, and 36.3 ± 1.8%, respectively. As several growth factors within the α-granules of the platelets are important for MSC proliferation and differentiation [33,34], the composition following production and storage is an important marker for platelet lysate quality. The effects of pathogen inactivation on growth factor stability during storage have previously been studied. It was demonstrated that UVC treatment of platelet concentrates had no effect on concentrations of EFG, FGF-2, PDGF-AB, VEGF, or IGF [35]. In a study specifically conducted on the INTERCEPT™ Blood System for pathogen inactivation, it was found that amotosalen plus UVA treatment mainly targets proteins of intracellular platelet activation pathways [36]. In addition, UV illumination of platelets combined with riboflavin or amotosalen seems to trigger activation of p38 mitogen-activated protein kinases (p38MAPK), leading to platelet degranulation [37]. However, to our knowledge this is the first study evaluating the effect of pathogen inactivation on lysed platelets compared to intact platelet concentrates. It can be speculated that, as a result of platelet cargo being released into solution of hPL-PIPL at the time of pathogen inactivation, the difference in composition between hPL-PIPC and hPL-PIPL is caused by UVA photodegradation, since light exposure can lead to irreversible changes in the primary, secondary, and tertiary structure of proteins [38].

As it has been suggested that hPL should contain high concentrations of PDGF-AB, VEGF, EGF, FGF-2, and TGF-β1, and low concentrations of IGF-1, we examined the long-term proliferation of MSCs from two donors in terms of cumulative population doublings (CPDs). Total CPDs were higher

for both of the donor hPL-PIPC-MSCs than for the hPL-PIPL-MSCs, indicating higher mitogenic effects in conventional hPL-PIPC. It is evident that EGF and VEGF activate the Raf-MEK-ERK pathway by binding to transmembrane receptor proteins at the plasma membrane [39]. Less activation of the Raf-MEK-ERK pathway may contribute to less cell proliferation and failure to prevent apoptosis. However, it is important to mention that high CPDs should not be viewed as a success criterion in isolation; successful expansion of MSCs must also include retention of genomic stability and avoidance of tumorigenicity [40].

Tri-lineage differentiation potential was examined *in vitro* by stimulating MSCs in osteogenic, adipogenic, and chondrogenic media. After 14 days of differentiation, both hPL-PIPC-MSCs and hPL-PIPL-MSCs differentiating into osteoblasts demonstrated significantly higher ALP activity compared to unstimulated control cultures. The presence of peak ALP levels around day 14 is a marker for osteogenic differentiation [41] and, in our study, indicated osteogenic differentiation potential. This was supported by mineralization and bone-like nodule formation after 28 days of differentiation in both treatments.

Adipogenic differentiation potential was evaluated over the course of 14 days. As mature adipocytes predominantly consist of lipid droplets [42], we used positive Oil Red O staining to visualize the transition from MSCs into adipocytes. Morphological alterations from spindle-shaped MSCs toward round adipocytes were observed after 7 days in both hPL types. Similarly, lipid droplets had formed at the periphery of the cells by day 7, and after 14 days the lipid droplets took up most of the intracellular space.

Finally, we evaluated chondrogenic differentiation potential over a period of 35 days. Cell pellets from both hPL-PIPC-MSCs and hPL-PIPL-MSCs had accumulated significantly more glycosaminoglycans (GAGs) after 28 days of differentiation than unstimulated control cultures. This was consistent at day 35 for hPL-PIPC-MSCs, whereas the GAG concentration decreased between days 28 and 35 for hPL-PIPL-MSCs. To evaluate changes within pellet structures, the pellets were sectioned and stained with Masson's trichrome. During differentiation, we observed lacunae formation and collagen fiber formation, which confirmed successful chondrogenic differentiation.

Based on the results obtained in this study, it appears that the application of pathogen inactivation techniques after platelet expiry may prove to be a valuable tool in the pursuit of optimal safety and standardization in therapeutic-grade human platelet lysate production.

Conclusions

In this study, we demonstrated that functional hPL can be produced by performing pathogen inactivation after platelet lysis of expired and previously untreated platelet concentrates (hPL-PIPL). hPL-PIPL successfully supported long-term cell proliferation and tri-lineage differentiation of BM-MSCs. While hPL-PIPL performed comparably to hPL-PIPC in terms of tri-lineage differentiation, lower cumulative population doublings (CPDs) were observed for hPL-PIPL. hPL-PIPL was also found to contain lower concentrations of key growth factors, suggesting that the timing of pathogen inactivation affects the mitogenic potential of hPL rather than differentiation potential.

Materials and methods

Preparation of platelet lysates

Four platelet concentrates (PCs) were prepared from a total of 32 buffy coats according to standard procedure at the Blood Bank, Landspitali (The National University Hospital of Iceland), Reykjavík, Iceland, as specified in Table 2. Two separate batches of PCs (batch nos. 23 and 24) were each prepared by pooling two buffy coat-derived PCs together. Each pooled batch represented 16 whole blood donations obtained from healthy donors of the Blood Bank. Each batch was further split into two units (and exposed to pathogen inactivation at different timepoints. The first unit, hPL-PIPC, was exposed to pathogen inactivation using the INTERCEPT™ Blood System (Cerus Corporation, Concord, CA, USA) less than 24 hours post donation, according to manufacturer's protocol. Following pathogen inactivation, the PCs were placed into a platelet agitator at 22 ± 2°C for seven days until expiration, and

then stored at -80°C for three weeks prior to platelet lysate production. The second unit, hPL-PIPL, was placed directly into the platelet agitator at 22 ± 2°C without being pathogen inactivated, stored for seven days until expiration, and then transferred to -80°C storage for three weeks. Pathogen inactivation for this second unit was performed after platelet lysis.

Table 2. Platelet concentrate characteristics.

PC No.	Number of buffy coats[a]			Mean platelet count ($\times 10^9$)	Batch no.
	Total	O+	O-		
1	8	7	1	278 ± 88.6	23
2	8	4	4	211 ± 50.5	23
3	8	8	0	197 ± 40.2	24
4	8	5	3	195 ± 25.4	24
Total	32	24	8	220 ± 34.1	

[a] Four buffy coat-derived platelet concentrates (PC) from donors with either O RhD positive (O+) or O RhD negative (O-) blood groups comprised the starting material.

The expired PCs were collected and subjected to platelet lysis by three cycles of thawing at 37°C and freezing at -80°C to initiate degranulation. After the third cycle, the platelet lysates were aliquoted in 50-mL centrifugation tubes (Corning Science, Reynosa Tamaulipas, Mexico). Platelet fragments were removed by centrifugation at 4975 × g for 20 minutes using a Heraeus Multifuge X3 (Thermo Scientific, Waltham, Massachusetts, USA). This centrifugation step was repeated after the supernatants (platelet lysates) from each tube were transferred to new 50-mL centrifugation tubes. Prepared lysates from each unit were pooled. The hPL-PIPC units were distributed into 45 mL aliquots and stored at -20°C in a freezer (Gram BioLine, Vojens, Denmark). In addition, 1 mL and 5 mL aliquots were prepared for composition analysis and adipogenic differentiation, respectively, and stored at -20°C prior to analysis. The hPL-PIPL units were injected into sterile bags (Cerus Corporation, Concord, CA, USA) and

297 exposed to pathogen inactivation with the INTERCEPT™ Blood System, according to the
298 manufacturer's protocol, before being aliquoted and stored at -20°C as above.
299 These undiluted platelet lysates were used for experimentation within 18 months of storage.
300

301 Growth factor and cytokine quantification

302 The undiluted platelet lysates were analyzed using Luminex xMAP Technology (EMD Millipore
303 Corporation, Billerica, MA, USA) to quantify 37 soluble growth factors and cytokines. The Human
304 Cytokine/Chemokine Magnetic Bead Panel (HCYTOMAG-60K, Millipore) was used; it applies
305 microspheres and fluorescent signaling to quantify EGF, Eotaxin, FGF-2, Fractalkine, G-CSF, GM-
306 CSF, IFNα2, IFNγ, IL-1α, IL-1β, IL-2, IL-3, IL-4, IL-5, IL-6, IL-7, IL-8, IL-9, IL-10, IL-12P40, IL-
307 12P70, IL-13, IL-15, IL-17A, IL-1RA, IP-10, MCP-1, MCP-3, MDC, MIP-1α, MIP-1β, PDGF-AA,
308 PDGF-AB/BB, TGF-α, TNFα, TNFβ, and VEGF. The concentrations in hPL-PIPL were compared to
309 those in hPL-PIPC and expressed as percentage difference in relation to hPL-PIPC (Equation 1, where
310 $[GF/C]_{hPL\text{-}PIPx}$ refers to the concentration of a particular growth factor or cytokine in the hPL-PIPC or
311 hPL-PIPL treatment).
312

$$\%\, Difference = \frac{[GF/C]_{hPL-PIPC} - [GF/C]_{hPL-PIPL}}{[GF/C]_{hPL-PIPC}} \cdot 100\% \quad (1)$$

313

314 Cell culturing

315 Mesenchymal stromal cells originating from the bone marrow of two healthy human donors were
316 purchased from Lonza (Walkersville, MD, USA) and stored at -180°C in liquid nitrogen prior to
317 experimentation. The cells tested negative for viral infections and mycoplasma. Prior to
318 experimentation, the MSCs were cultured in a cell culture medium supplemented with hPL-PIPC
319 through passage 3. Subsequently, the MSCs were distributed into two cell culture flasks supplemented
320 with either hPL-PIPC or hPL-PIPL at the time of cell split (between passage 3 and passage 4). MSCs in
321 passage 5 were used for experimentation.

The culture medium used was a complete cell culture medium (referred to as "expansion medium" in this study) consisting of Dulbecco's Modified Eagle Medium (DMEM) / F12 + Glutamax supplement (Gibco, Grand Island, NY, USA) with 1% penicillin/streptomycin (Gibco) and 2 IU/mL heparin (Leo Pharma A/S, Ballerup, Denmark), supplemented with a sufficient amount of either hPL-PIPC (to produce hPL-PIPC-MSCs) or hPL-PIPL (to produce hPL-PIPL-MSCs) to achieve a final concentration of 9%. Specifically, after allowing solutions to reach ambient temperature, 50 mL of platelet lysate was centrifuged at 4975 × g for 10 minutes and added to 500 mL DMEM / F12 + Glutamax along with 5 mL of penicillin/streptomycin and 200 µL heparin. The medium was allowed to sit for 10 minutes prior to sterile filtration. Sterile filtration was performed using a 0.45 µm low protein-binding funnel (Corning Incorporated, NY, USA) in a closed system. Finally, the medium was aliquoted into 45-mL centrifugation tubes (Corning Incorporated) and stored at -20°C until use. Once thawed for use in cell cultures, the medium was maintained at 4°C in a laboratory refrigerator (Angelantoni Life Sciences, Massa Martana, Italy) for a maximum of seven days.

Incubation was done in a Steri-Cult CO2 Incubator, HEPA Class 100 (Thermo Scientific) under the following conditions: 37°C; 5% CO^2, and 95% humidity.

Cell expansion was performed in different vessels appropriately selected for each experiment at a seeding density of 6000 cells/cm^2. For the initial cell expansion prior to experimentation, MSCs were expanded in 20 mL of expansion medium in Nunc™ EasYFlask™ 75 cm^2 (T75) cell culture flasks (Thermo Fischer Scientific Nunc A/S, Roskilde, Denmark). For long-term proliferation studies, MSCs were expanded in 5 mL of expansion medium in Nunc™ EasYFlask™ 25 cm^2 (T25) cell culture flasks (Thermo Fischer Scientific Nunc A/S). In both cases, the expansion medium was replaced every two to three days.

Cell passaging was performed upon reaching 80-90% confluency, as determined visually by daily inspection using a Leica DM IRB inverted contrast microscope (Leica Microsystems, Wetzlar, Germany). In brief, the MSCs were gently washed with 1X PBS (Gibco) and dissociated from the surface in 0.25% 1X Trypsin-EDTA (Gibco) for 5 minutes. Preheated expansion medium was added to neutralize the trypsin-EDTA before the cells were centrifuged at 609 × g for 5 minutes. After

centrifugation, the supernatant was discarded and the pellet was carefully resuspended in 1 mL preheated medium prior to cell counting. The cells were diluted 5X by mixing 20 µL resuspended cells, 30 µL 1X PBS, and 50 µL 0.4% trypan blue stain (Gibco) in a 1.5-mL micro tube (SARSTEDT AG & Co., Nümbrecht, Germany). The cell solution was loaded onto a hemocytometer (BRAND GMBH + CO KG, Wertheim, Germany), covered by a glass, and counted at 50X magnification. Viable MSCs were identified by the retention of their round morphology and by their lack of trypan blue uptake. Viable MSCs located in the four corner squares were counted twice using the upper and lower chambers and averaged to estimate the number of cells. If the sum of the four corner squares in a single chamber exceeded 200 viable MSCs, the cell solution was diluted further and the cell count repeated. Cell passaging was completed by seeding 6000 cells/cm^2 into a new cell culture vessel.

Long-term proliferation was evaluated by expanding and passaging MSCs in T25 cell culture flasks. Initially, MSCs entering passage 5 were seeded into six T25 cell culture flasks and expanded in cell culture media supplemented with either hPL-PIPC or hPL-PIPL. The expansion medium was replaced every two to three days, and cell passaging was carried out upon reaching 80-90% confluency. All cell culture flasks were passaged on the same day and the number of population doublings (PDs) was determined using Equation 2, where N0 and N1 represent the number of cells seeded and cells harvested, respectively.

$$PDs = \frac{\log_{10}(N0) - \log_{10}(N1)}{\log_{10}(2)} \quad (2)$$

Cumulative population doublings (CPDs) were expressed as the sum of the PDs obtained in each passage. Cell expansion was terminated upon achieving recovery rates of less than 100% of the seeded cell number after a maximum of 14 days in culture. Daily monitoring was performed to assess morphological alterations.

Tri-lineage differentiation

MSCs in passage 5 were used to evaluate *in vitro* tri-lineage differentiation potential. Osteogenic and adipogenic differentiation were performed simultaneously using the same cell cultures. Chondrogenic differentiation was performed separately due to the large number of required cells.

Osteogenic differentiation

Osteogenic differentiation was evaluated at various timepoints during 28 days of stimulation in osteogenic medium. The osteogenic medium consisted of 45 mL DMEM / F12 + Glutamax (Gibco) supplemented with 5 mL platelet lysate, 50 µL dexamethasone (Sigma-Aldrich, St. Louis, MO, USA), 50 µL human/murine/rat BMP-2 (Peprotech, Rocky Hill, NJ, USA), 50 µL L-ascorbic acid (Sigma-Aldrich), and 108 mg β-glycerophosphate disodium salt hydrate (Sigma-Aldrich). An increase in alkaline phosphatase activity and positive staining for mineralization were used as markers. In brief, 3500 cells/cm^2 were seeded in quadruplicate in 6-well tissue culture plates (Corning Incorporated) and in triplicate in 12-well tissue culture plates (Corning Incorporated) for each timepoint. Control plates were included by seeding 5500 cells/cm^2 in expansion media in absence of osteogenic stimulation. Plates were incubated at 37°C, 5% CO^2, and 95% humidity for up to 28 days. The cell culture medium was replaced every two to three days. The left half of the 12-well plates was used to quantify ALP activity, while the right half was used to detect mineralization by staining with Alizarin Red S.

Enzymatic activity of ALP was evaluated after 7, 14, 21, and 28 days of osteogenic differentiation. Briefly, 0.02% Triton-X (Sigma-Aldrich) diluted in 1X PBS was added to all samples, and then the cells were scraped off the surface and transferred to a 1.5-mL micro tube. The cells were vortexed and then centrifuged at 13,200 × g for 15 minutes at 4°C. After centrifugation, the supernatant was transferred to a new micro tube and mixed with 500 µL of p-nitrophenyl phosphate (pNPP) solution, prepared using SIGMAFAST™ pNPP and SIGMAFAST™ Tris Buffer (Sigma-Aldrich). Next, the solution was incubated for 45 minutes at 37°C protected from light, and the absorbance was measured at 400 nm. Each sample reading was corrected by the average absorbance of three blank replicates. ALP activity (nmol (p-nitrophenol)/min) was calculated using Equation 3,

$$activity = \frac{OD/18.8}{t} \cdot 1000\,, \tag{3}$$

where OD refers to the optical density obtained at 400 nm (-), 18.8 is the extinction coefficient of p-nitrophenol (μmol^{-1}), t is time (min), and 1000 is used to convert µmol to nmol.

Alizarin Red S staining was performed to visualize mineralization during osteogenic differentiation. Cell cultures were collected and fixed in 4% paraformaldehyde after 7, 14, 21, and 28 days of osteogenic differentiation and stored at 4°C prior to staining. Cells were washed three times with distilled water (dH_2O) before adding a 2% Alizarin Red solution containing Alizarin Red S dye (Sigma-Aldrich) diluted in dH_2O. The cells were placed on a rotating shaker and stained for 20 minutes at room temperature, followed by four washing steps using dH_2O. The dye was allowed to dry for 24 hours by inverting the plates on paper towels. The following day, images were captured using inverted contrast microscope imaging, and alterations in morphology and formation of bone-like nodules were evaluated.

Adipogenic differentiation

Adipogenic differentiation was evaluated after 7 and 14 days of stimulation in adipogenic medium. Adipogenic medium consisted of 22.5 mL StemPro® Adipocyte Differentiation Basal Medium (Gibco), 2.5 mL StemPro® Adipogenesis Supplement (Gibco), 0.25 mL penicillin/streptomycin, 2.5 mL platelet lysate, and 20 µL heparin.

In brief, 10,000 cells/cm^2 were seeded in triplicate Nunc™ 9 cm^2 Slideflasks (Thermo Fischer Scientific Nunc A/S). Control slideflasks were included by seeding 5500 cells/cm^2 in expansion media in absence of adipogenic stimulation. Sideflasks were incubated at 37°C, 5% CO^2, and 95% humidity for up to 14 days. The MSCs were allowed to reach a confluency of 50-70% in expansion media prior to introduction of the adipogenic medium. The cell culture medium was replaced every two to three days. Cultures in the 9 cm^2 slideflasks were washed three times in 1X PBS and fixed in 3 mL of 4% paraformaldehyde and stored at 4 °C after 7 or 14 days prior to Oil Red O staining.

Upon termination of the experiment, the slideflasks were collected and sent to the Department of Pathology (Landspitali, Háskólasjúkrahús, Reykjavík, Iceland) where Oil Red O staining was performed according to departmental protocols. Positive Oil Red O-stained lipid droplets were used as markers of adipogenic differentiation.

Chondrogenic differentiation

Chondrogenic differentiation was evaluated after 14, 28, and 35 days of stimulation in chondrogenic medium. Chondrogenic medium consisted of 47.9 mL DMEM / F12 + Glutamax supplemented with 9% hPL, 1% penicillin/streptomycin, 50 µL L-ascorbic acid, 50 µL dexamethasone, 500 µL sodium pyruvate (Sigma-Aldrich), 500 µL L-proline (Sigma-Aldrich), 500 µL ITS+ (Gibco) and 5 µL of 10 ng/µL TGF-β3. Production of glycosaminoglycans, as well as positive collagen fibers and lacunae formation visualized by chondrocytic pellet staining with Masson's trichrome were used as markers of chondrogenic differentiation.

In brief, 250,000 cells were seeded in ten 1.5-mL micro tubes containing 0.5 mL chondrogenic media for each timepoint. Control micro tubes were included by seeding 250,000 cells in expansion media in absence of chondrogenic stimulation. Pellets were formed by centrifugation at 152 × g using a Sorvall Instruments RC5C centrifuge (Thermo Fischer Scientific). The caps were punctured with a sterile needle to allow air exchange, and the tubes were incubated at 37°C, 5% CO^2, and 95% humidity for up to 35 days. After 18-24 hours, the tubes were gently agitated to detach the pellets from the wall of the micro tubes. To minimize the stress on the pellets, half of the cell culture medium was replaced every second day. At each sampling timepoint (14, 28, and 35 days), three pellets were analyzed for GAG content and two pellets were prepared for histological staining.

To prepare pellets for the GAG assay, the three pellets were pooled into a micro tube containing 500 µL papain extraction reagent (Sigma-Aldrich). The samples were then transferred to a Grant-Bio PHMT heating block (Grant Instruments Ltd, Shepreth, Cambridgeshire, UK) and fully digested at 65°C for a maximum of seven hours. After digestion, the samples were centrifuged at 9660 × g and the supernatants were transferred to new micro tubes and stored at -80°C.

453 To prepare pellets for histological staining, the pellets were collected and washed in 1X PBS prior
454 to fixation in 0.5 mL 4% paraformaldehyde in new micro tubes. The samples were stored at 4°C prior
455 to histological staining.

456 The Biocolor Blyscan Sulfated Glycosaminoglycan Assay B1000 (Biocolor Ltd, County Antrim,
457 United Kingdom) was used to quantify the concentrations of GAGs. The assay was performed according
458 to the manufacturer's protocol. In brief, standards diluted in papain extraction reagent were prepared
459 containing GAGs in the working range of 0-5 µg/mL. 1 mL of Blyscan dye reagent was added to a new
460 micro tube prepared for each standard and sample. 100 µL of each standard and sample was then added
461 to the new micro tubes and mixed with the Blyscan dye reagent for 30 minutes on a mechanical shaker
462 (Heidolph, Schwabach, Germany). After incubation, the micro tubes were centrifuged for 10 minutes at
463 9660 × g. The supernatant was separated from the pellet by inverting the micro tubes carefully before
464 adding 0.5 mL dissociation reagent. Prior to quantification, the micro tubes were vortexed to release
465 bound dye into the solution. 200 µL of each standard and sample was loaded into a 96-well tissue culture
466 plate in triplicate and measured at 656 nm using a Multiskan® spectrum spectrophotometer (Thermo
467 Scientific, Vantaa, Finland). The average absorbance of the blank replicates was subtracted from each
468 standard and sample. The GAG concentration of each sample was determined using the standard curve.
469 To express GAG concentration per pellet, the values were divided by three to account for the number of
470 pooled pellets.

471 Upon experimental termination, the micro tubes were collected and sent to the Department of
472 Pathology (Landspitali, Háskólasjúkrahús, Reykjavík, Iceland). Masson's trichrome and hematoxylin
473 and eosin staining were performed according to departmental protocols.

474

475 Statistical analysis

476 Statistical comparisons were performed using GraphPad Prism Version 7.04 software (GraphPad
477 Software, Inc., San Diego, CA, USA). Paired t-tests were performed to analyze differences in total
478 protein. Ratio paired t-tests were performed to analyze differences in the content of growth factors and
479 cytokines. Differences in proliferation and differentiation were analyzed using a two-way ANOVA

480 followed by multiple comparisons using Tukey's post hoc test. Differences were considered significant
481 at $p < 0.05$.

482 The sample size (N) for each experiment refers to the number of experimental units derived from
483 biological units using separate cell culture vessels. Nomenclature and principle were adapted from Lazic
484 et al. [43].

485

486 Acknowledgements

487 We would like to thank Ragna Landrö for processing the platelet concentrates and Sigrún Bærings
488 Kristjánsdóttir for support with staining procedures.

References

1. Allain JP, Bianco C, Blajchman MA, Brecher ME, Busch M, Leiby D, et al. Protecting the blood supply from emerging pathogens: the role of pathogen inactivation. Transfus Med Rev. 2005;19(2):110–26.
2. Drew VJ, Barro L, Seghatchian J, Burnouf T. Towards pathogen inactivation of red blood cells and whole blood targeting viral DNA/RNA: design, technologies, and future prospects for developing countries. Blood Transfus. 2017;15(6):512–21.
3. Irsch J, Lin L. Pathogen inactivation of platelet and plasma blood components for transfusion using the INTERCEPT Blood System™. Transfus Med Hemother. 2011;38(1):19–31.
4. Green L, Allard S, Cardigan R. Modern banking, collection, compatibility testing and storage of blood and blood components. Anaesthesia. 2015;70(Suppl 1):3-9,e2.
5. Bakkour S, Chafets DM, Wen L, Dupuis K, Castro G, Green JM, et al. Assessment of nucleic acid modification induced by amotosalen and ultraviolet A light treatment of platelets and plasma using real-time polymerase chain reaction amplification of variable length fragments of mitochondrial DNA. Transfusion. 2016;56(2):410–20.
6. Ellingson KD, Sapiano MRP, Haass KA, Savinkina AA, Baker ML, Chung KW, et al. Continued decline in blood collection and transfusion in the United States–2015. Transfusion. 2017;57(Suppl 2):1588–98.
7. Guan L, Tian X, Gombar S, Zemek AJ, Krishnan G, Scott R, et al. Big data modeling to predict platelet usage and minimize wastage in a tertiary care system. Proc Natl Acad Sci U S A. 2017;114(43):11368–73.
8. Jonsdottir-Buch SM, Lieder R, Sigurjonsson OE. Platelet lysates produced from expired platelet concentrates support growth and osteogenic differentiation of mesenchymal stem cells. PLoS ONE. 2013;8(7):e68984.
9. Caplan AI. Adult mesenchymal stem cells for tissue engineering versus regenerative medicine. J Cell Physiol. 2007;213(2):341–7.

10. Friedenstein AJ, Petrakova KV, Kurolesova AI, Frolova GP. Heterotopic of bone marrow. Analysis of precursor cells for osteogenic and hematopoietic tissues. Transplantation. 1968;6(2):230–47.
11. Bara JJ, Richards RG, Alini M, Stoddart MJ. Concise review: Bone marrow-derived mesenchymal stem cells change phenotype following in vitro culture: implications for basic research and the clinic. Stem Cells. 2014;32(7):1713–23.
12. Abdi R, Fiorina P, Adra CN, Atkinson M, Sayegh MH. Immunomodulation by mesenchymal stem cells. Diabetes. 2008;57(7):1759–67.
13. Wang L, Zhu C, Ma D, Gu Z, Xu C, Wang F, et al. Efficacy and safety of mesenchymal stromal cells for the prophylaxis of chronic graft-versus-host disease after allogeneic hematopoietic stem cell transplantation: a meta-analysis of randomized controlled trials. Ann Hematol. 2018;97(10):1941–50.
14. Phinney DG. Biochemical heterogeneity of mesenchymal stem cell populations: clues to their therapeutic efficacy. Cell Cycle. 2007;6(23):2884–9.
15. Squillaro T, Peluso G, Galderisi U. Clinical trials with mesenchymal stem cells: an update. Cell Transplant. 2016 May 1;25(5):829–48.
16. van der Valk J, Bieback K, Buta C, Cochrane B, Dirks WG, Fu J, et al. Fetal bovine serum (FBS): past - present - future. ALTEX. 2018;35(1):99-118.
17. Gstraunthaler G. Alternatives to the use of fetal bovine serum: serum-free cell culture. ALTEX. 2003;20(4):275–81.
18. van der Valk J, Mellor D, Brands R, Fischer R, Gruber F, Gstraunthaler G, et al. The humane collection of fetal bovine serum and possibilities for serum-free cell and tissue culture. Toxicol In Vitro. 2004;18(1):1–12.
19. Flemming A, Schallmoser K, Strunk D, Stolk M, Volk H-D, Seifert M. Immunomodulative efficacy of bone marrow-derived mesenchymal stem cells cultured in human platelet lysate. J Clin Immunol. 2011;31(6):1143–56.
20. Bieback K. Platelet lysate as replacement for fetal bovine serum in mesenchymal stromal cell cultures. Transfus Med Hemother. 2013;40(5):326–35.

543 21. Burnouf T, Strunk D, Koh MBC, Schallmoser K. Human platelet lysate: replacing fetal bovine
544 serum as a gold standard for human cell propagation? Biomaterials. 2016;76(Suppl C):371–87.
545 22. Jonsdottir-Buch SM, Sigurgrimsdottir H, Lieder R, Sigurjonsson OE. Expired and pathogen-
546 inactivated platelet concentrates support differentiation and immunomodulation of mesenchymal
547 stromal cells in culture. Cell Transplant. 2015;24(8):1545–54.
548 23. Astori G, Amati E, Bambi F, Bernardi M, Chieregato K, Schäfer R, et al. Platelet lysate as a
549 substitute for animal serum for the ex-vivo expansion of mesenchymal stem/stromal cells: present
550 and future. Stem Cell Res Ther. 2016;7(1):93.
551 24. Doucet C, Ernou I, Zhang Y, Llense J-R, Begot L, Holy X, et al. Platelet lysates promote
552 mesenchymal stem cell expansion: a safety substitute for animal serum in cell-based therapy
553 applications. J Cell Physiol. 2005;205(2):228–36.
554 25. Copland IB, Garcia MA, Waller EK, Roback JD, Galipeau J. The effect of platelet lysate fibrinogen
555 on the functionality of MSCs in immunotherapy. Biomaterials. 2013;34(32):7840–50.
556 26. Bernardi M, Albiero E, Alghisi A, Chieregato K, Lievore C, Madeo D, et al. Production of human
557 platelet lysate by use of ultrasound for ex vivo expansion of human bone marrow–derived
558 mesenchymal stromal cells. Cytotherapy. 2013;15(8):920–9.
559 27. Shih DT-B, Burnouf T. Preparation, quality criteria, and properties of human blood platelet lysate
560 supplements for ex vivo stem cell expansion. N Biotechnol. 2015;32(1):199–211.
561 28. Rauch C, Feifel E, Amann EM, Spötl HP, Schennach H, Pfaller W, et al. Alternatives to the use of
562 fetal bovine serum: human platelet lysates as a serum substitute in cell culture media. ALTEX.
563 2011;28(4):305–16.
564 29. Strunk D, Lozano M, Marks DC, Loh YS, Gstraunthaler G, Schennach H, et al. International forum
565 on GMP-grade human platelet lysate for cell propagation: summary. Vox Sang. 2018;113(1):80-7.
566 30. Viau S, Lagrange A, Eap S, Chabrand L, Lorant J, Charrier M, et al. A standardized and
567 characterized clinical grade human platelet lysate for efficient expansion of human bone marrow
568 mesenchymal stem cells. Cytotherapy. 2018;20(5, Supplement):S54.

569 31. Chou ML, Burnouf T. Current methods to manufacture human platelet lysates for cell therapy and
570 tissue engineering: possible trends in product safety and standardization. ISBT Sci Ser.
571 2017;12(1):168–75.
572 32. Pietersz RNI, Reesink HW, Panzer S, Oknaian S, Kuperman S, Gabriel C, et al. Bacterial
573 contamination in platelet concentrates. Vox Sang. 2014;106(3):256–83.
574 33. Ng F, Boucher S, Koh S, Sastry KSR, Chase L, Lakshmipathy U, et al. PDGF, TGF-β, and FGF
575 signaling is important for differentiation and growth of mesenchymal stem cells (MSCs):
576 transcriptional profiling can identify markers and signaling pathways important in differentiation of
577 MSCs into adipogenic, chondrogenic, and osteogenic lineages. Blood. 2008;112(2):295–307.
578 34. Lykov AP, Bondarenko NA, Surovtseva MA, Kim II, Poveshchenko OV, Pokushalov EA, et al.
579 Comparative effects of platelet-rich plasma, platelet lysate, and fetal calf serum on mesenchymal
580 stem cells. Bull Exp Biol Med. 2017;163(6):757–60.
581 35. Viau S, Chabrand L, Eap S, Lorant J, Rouger K, Goudaliez F, et al. Pathogen reduction through
582 additive-free short-wave UV light irradiation retains the optimal efficacy of human platelet lysate
583 for the expansion of human bone marrow mesenchymal stem cells. PLoS ONE.
584 2017;12(8):e0181406.
585 36. Prudent M, D'Alessandro A, Cazenave JP, Devine DV, Gachet C, Greinacher A, et al. Proteome
586 changes in platelets after pathogen inactivation—an interlaboratory consensus. Transfus Med Rev.
587 2014;28(2):72–83.
588 37. Schubert P, Johnson L, Marks DC, Devine DV. Ultraviolet-based pathogen inactivation systems:
589 untangling the molecular targets activated in platelets. Front Med. 2018;5:129.
590 38. Kerwin BA, Remmele RL. Protect from light: photodegradation and protein biologics. J Pharm Sci.
591 2007;96(6):1468–79.
592 39. Zhang W, Liu HT. MAPK signal pathways in the regulation of cell proliferation in mammalian
593 cells. Cell Res. 2002;12(1):9–18.
594 40. Wang S, Qu X, Zhao RC. Clinical applications of mesenchymal stem cells. J Hematol Oncol.
595 2012;5:19.

596 41. Birmingham E, Niebur GL, McHugh PE, Shaw G, Barry FP, McNamara LM. Osteogenic
597 differentiation of mesenchymal stem cells is regulated by osteocyte and osteoblast cells in a
598 simplified bone niche. Eur Cell Mater. 2012;23:13–27.
599 42. Lowe CE, O'Rahilly S, Rochford JJ. Adipogenesis at a glance. J Cell Sci. 2011;124(16):2681–6.
600 43. Lazic SE, Clarke-Williams CJ, Munafò MR. What exactly is 'N' in cell culture and animal
601 experiments? PLoS Biol. 2018;16(4):e2005282.
602

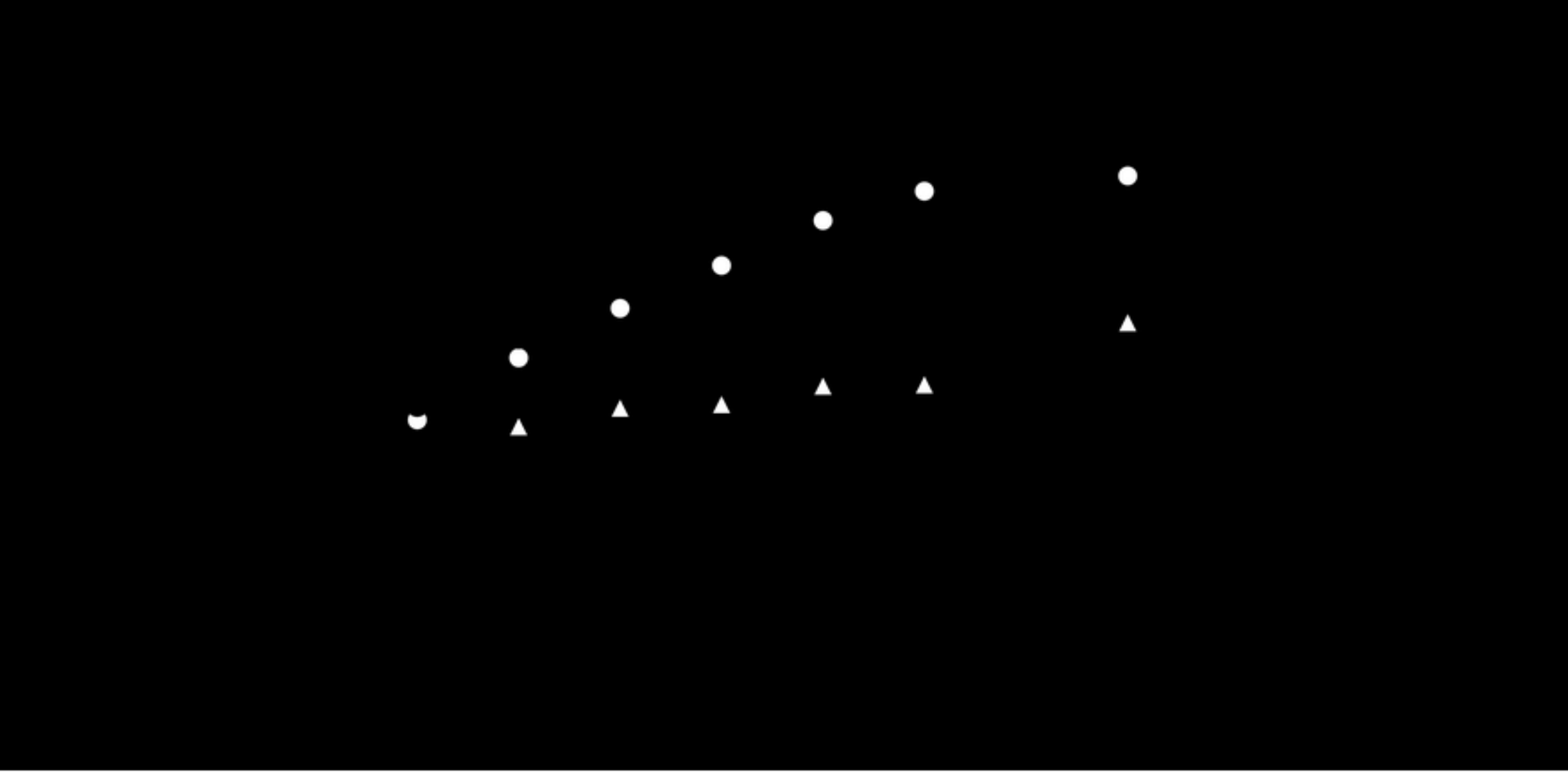

Figure 1

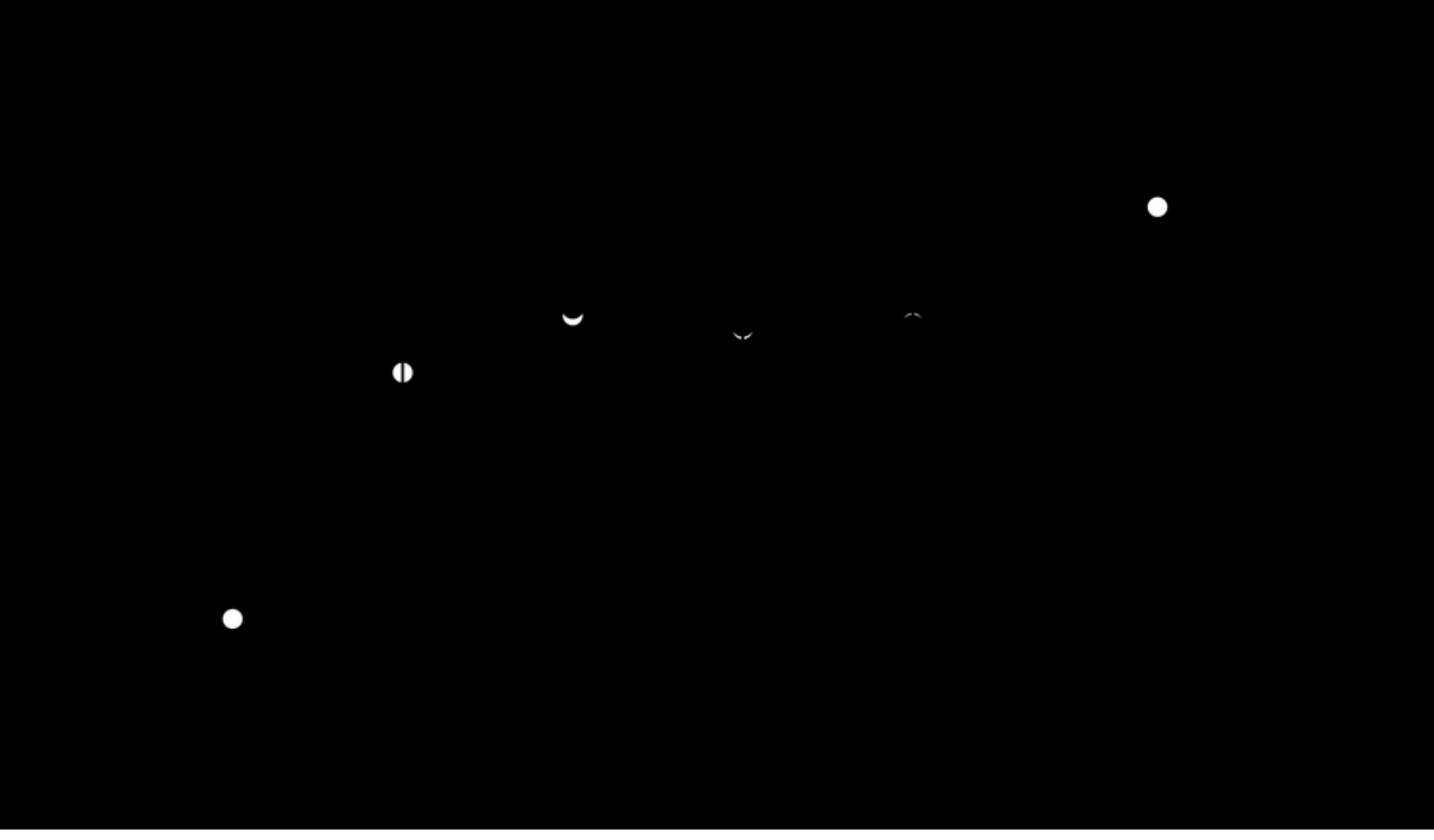

Figure2

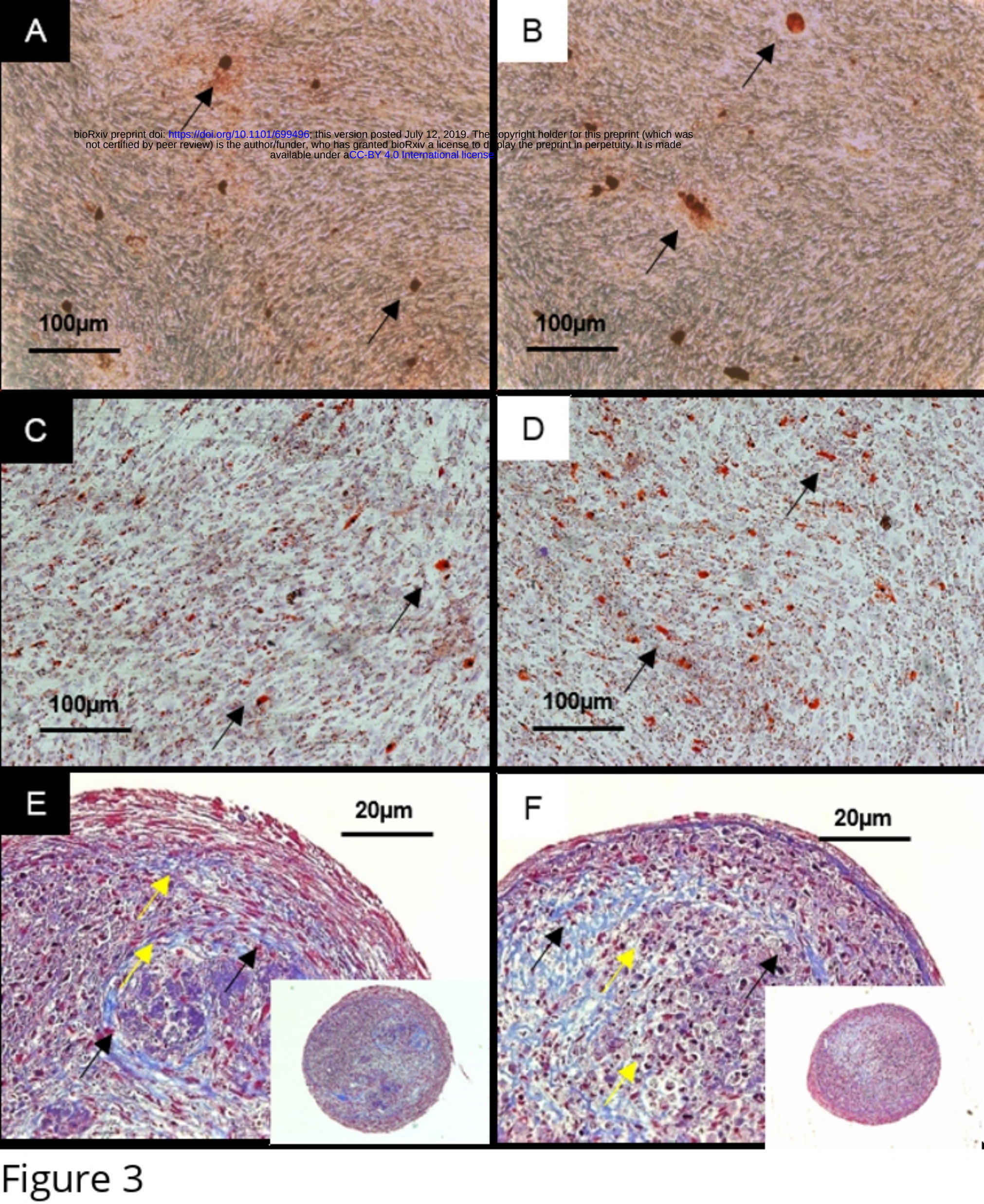

Figure 3

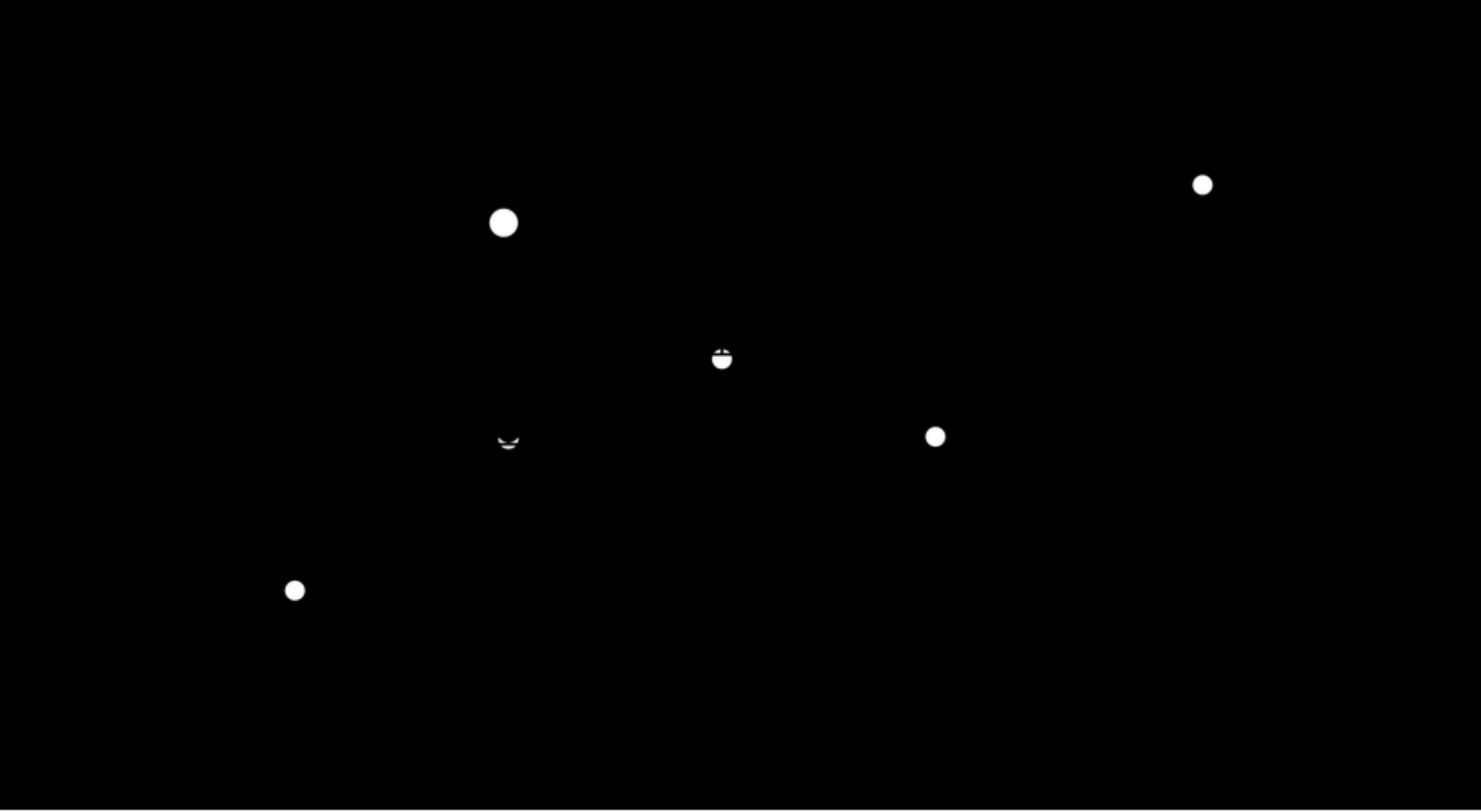

Figure 4